The 2nd Joint International Conference on Multibody System Dynamics
May 29–June 1, 2012, Stuttgart, Germany

Planned contacts and collision avoidance in optimal control problems

Sigrid Leyendecker*, Gwen Johnson#, Michael Ortiz#

* Chair of Applied Dynamics
University of Erlangen-Nuremberg
Konrad-Zuse-Straße 3-5, 91052 Erlangen, Germany
sigrid.leyendecker@ltd.uni-erlangen.de

Computational Solid Mechanics Group
California Institute of Technology
MC 105-50, Pasadena CA 91125
gwen@caltech.edu, ortiz@aero.caltech.edu

ABSTRACT

In previous works, discrete mechanics and optimal control for constrained systems (DMOCC) has been introduced for the structure preserving simulation of optimal control problems for rigid multibody systems, whereby possible contacts or collisions between the bodies have been disregarded. In the formulation presented here, both collision avoidance as well as explicitly planned collisions between non-smooth bodies are included. To this end, a subdifferentiable global contact detection algorithm, the supporting separating hyperplane linear program (SSHLP), based on the signed distance between supporting hyperplanes of two convex sets, is used in the simulation of optimal control problems.

1 INTRODUCTION

When simulating the dynamics of three-dimensional multibody systems, the treatment of contact always imposes a challenge. One simple solution is to formulate a smooth problem where the bodies are allowed to overlap by a certain amount, which is penalised via a penalty potential. Of course, the drawbacks of inadmissible configurations and inexact contact forces that go along with this approach are obvious. However, for the forward dynamics simulation of many applications, the results might be accurate enough, in particular when high penalty parameters in combination with small time steps are tolerable from the computational effort's point of view. If the bodies are not supposed to overlap, the discrete event of contact has to be considered as part of the system's dynamics, thus making the dynamics non-smooth. See e.g. [1, 3, 5, 10, 11] and many references on contact formulations in different contexts therein.

Non-smooth formulations require the specification of a contact force that (for elastic collisions) reflects the momentum normal to a contact surface at a given time and configuration. In the context of a structure preserving time integration method (being consistent in the evolution of energy and momentum maps) that uses a predefined equidistant time grid, there is no other known procedure except for resolving the collisions in the sense that each contact time (which is likely between the nodes), configuration, and force are exactly computed, see [2, 8].

This work will show how the described alternatives for the treatment of collisions can be included in the context of optimal control problems. In the smooth formulation with a penalty potential, there arises some difficulty for the optimiser to distinguish between a contact and a control force, since both might point into the same direction. For the non-smooth treatment, the optimal control problem formulation gives more freedom than the forward dynamics problem, since periodic boundary conditions or leaving the exact placement of time nodes (within certain bounds) to the optimiser gives the freedom to assume that contact takes place at a certain time node without loss of generality, i.e. without fixing its physical time. A further challenge is the detection of contact for non-smooth non-convex three-dimensional bodies where a new strategy based on a supporting separating hyperplane linear programming (SSHLP) approach is used, see [4]. One major advantage of this strategy is that the subgradient of the SSHLP, supplying the direction of the contact force, can be readily evaluated. Reconfiguration manoeuvres with collision avoidance and with planned collisions are considered as examples.

2 OPTIMAL CONTROL WITH COLLISION AVOIDANCE

In order to avoid collisions or even any contact between bodies (including grazing collisions, i.e. the mere touching contact without a velocity component in the direction normal to the contact surface), the first step is to detect contact or overlapping. This can be quite a challenge for three-dimensional non-smooth and maybe non-convex bodies. Then, the second step is to enforce the avoidance of collisions in the simulation of optimal control problems.

2.1 Contact detection for non-smooth bodies via SSHLP

To detect contact between convex bodies, a subdifferentiable global contact detection algorithm, the so called supporting separating hyperplane (SSH) algorithm, developed in [4] is used. Based on theorems from convex and affine geometry, this algorithm determines the signed distance between supporting hyperplanes of two convex sets. In its first formulation, the algorithm yields a quadratically constrained linear program. However, the problems's structure is such that an equivalent linear program (LP) (with explicit expressions of the subderivative supplying the contact force) can always be formulated.

For the positive integer n, let $\boldsymbol{\alpha} \neq \mathbf{0} \in \mathbb{R}^n$ and $a \in \mathbb{R}$, then the affine and convex set

$$H_{\boldsymbol{\alpha},a} = \{\boldsymbol{x} \in \mathbb{R}^n | \, \langle \boldsymbol{\alpha}, \boldsymbol{x} \rangle - a = 0\}$$

is called a hyperplane in $\mathbb{R}^n$. Here, $\boldsymbol{\alpha}$ is the normal vector to the plane while $a = \langle \boldsymbol{\alpha}, \boldsymbol{a} \rangle$ for some point $\boldsymbol{a} \in \mathbb{R}^n$ belonging to the plane. The signed distance between a point $\boldsymbol{y} \in \mathbb{R}^n$ and a hyperplane can be computed as $\langle \boldsymbol{\alpha}, \boldsymbol{y} \rangle - a$. Clearly, a hyperplane has two distinct sides. For $\boldsymbol{b} \in \mathbb{R}^n$ and $b = \langle \boldsymbol{\alpha}, \boldsymbol{b} \rangle$, the signed distance between parallel hyperplanes with normal $\boldsymbol{\alpha}$ reads $d(H_{\boldsymbol{\alpha},a}, H_{\boldsymbol{\alpha},b}) = b - a$.
Let $K_1, K_2 \subset \mathbb{R}^n$ be compact convex sets and let $\mathrm{ext}K_1, \mathrm{ext}K_2$ denote the sets of their extreme points (corners for polyhedral sets) and $\mathrm{bd}K_1, \mathrm{bd}K_2$ their boundaries, respectively. A hyperplane $H_{\boldsymbol{\alpha},a}$ is said to support the set K_1 at $\boldsymbol{x} \in \mathrm{bd}K_1$, when $\boldsymbol{x} \in H_{\boldsymbol{\alpha},a}$ and K_1 is entirely contained in one of the half-spaces associated with distinct sides of $H_{\boldsymbol{\alpha},a}$, i.e. for all $\boldsymbol{y} \in K_1$ either $\langle \boldsymbol{\alpha}, \boldsymbol{y} \rangle - a \leq 0$ or $\langle \boldsymbol{\alpha}, \boldsymbol{y} \rangle - a \geq 0$ holds.

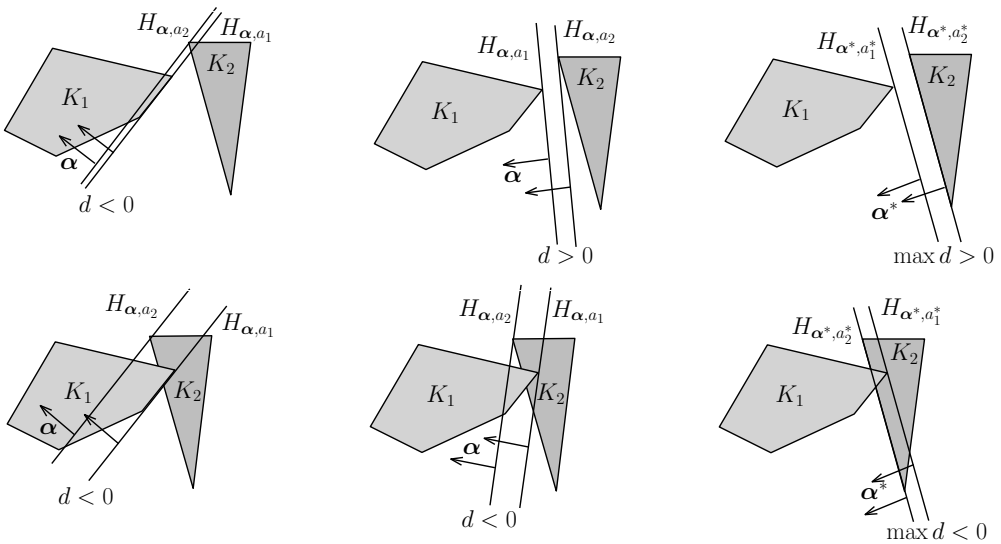

Figure 1. Strictly separable (first row) and non-separable (second row) polyhedral sets K_1, K_2 with signed distance between different supporting hyperplanes and maximum signed distance (Figure from [4]).

The maximum signed distance between parallel supporting hyperplanes of each set can be computed either as a solution $h(K_1, K_2)$ of the following quadratically constrained liner program (QCLP), or as the solution $g(K_1, K_2)$ of the following linearly constrained linear program (LCLP) for some unit vector $\boldsymbol{\beta} \in S^{n-1}$.

QCLP	LCLP
$h(K_1,K_2) = \max\limits_{\substack{\boldsymbol{\alpha}\in\mathbb{R}^n \\ a_1,a_2\in\mathbb{R}}} a_1 - a_2$	$g(K_1,K_2) = \max\limits_{\substack{\boldsymbol{\alpha}\in\mathbb{R}^n \\ a_1,a_2\in\mathbb{R}}} a_1 - a_2$
subject to $\langle \boldsymbol{\alpha}, \boldsymbol{x}\rangle - a_1 \geq 0 \quad \forall\, \boldsymbol{x} \in \text{ext}K_1$	subject to $\langle \boldsymbol{\alpha}, \boldsymbol{x}\rangle - a_1 \geq 0 \quad \forall\, \boldsymbol{x} \in \text{ext}K_1$
$\langle \boldsymbol{\alpha}, \boldsymbol{y}\rangle - a_2 \leq 0 \quad \forall\, \boldsymbol{y} \in \text{ext}K_2$	$\langle \boldsymbol{\alpha}, \boldsymbol{y}\rangle - a_2 \leq 0 \quad \forall\, \boldsymbol{y} \in \text{ext}K_2$
$\langle \boldsymbol{\alpha}, \boldsymbol{\alpha}\rangle = 1$	$\langle \boldsymbol{\beta}, \boldsymbol{\alpha}\rangle = 1$

Using of the following three results shown in [4]

i) **Theorem 1**. *Two compact convex sets K_1 and K_2 are strictly separable, i.e. $K_1 \cap K_2 = \emptyset$ (properly separable, i.e. $K_1 \cap K_2 = \emptyset$ or $K_1 \cap K_2 \subset H_{\boldsymbol{\alpha},a_1} \equiv H_{\boldsymbol{\alpha},a_2}$) if and only if $h > 0$ (if and only if $h \geq 0$).*

ii) **Theorem 2**, giving conditions under which an optimal solution of the QCLP is equivalent to an optimal solution of the LCLP

iii) **Remark 3** and remarks following the proof of Theorem 2 on the choice of $\boldsymbol{\beta}$ in praxis

we solve the LCLP to detect contact or overlapping between non-smooth convex bodies. If non-convex bodies are present, they are subdivided into convex bodies for which then contact or overlapping is tested.

2.2 Discrete mechanics and optimal control for constrained systems with collision avoidance

The goal of an optimal control problem is to determine an optimal state trajectory with the corresponding optimal control trajectory actuating the dynamical system such that an optimality criterion is reached. Thus, an objective functional is minimised with respect to the state and control trajectory while the equations of motion, initial and final conditions as well as path constraints have to be fulfilled. To simulate an optimal control problem numerically via a direct method, the problem is transformed into a finite dimensional constrained optimisation problem which can be solved e.g. by a standard SQP or interior point method. Thereby, the particular form of the discrete equations of motion (which serve as constraints for the optimisation) plays a crucial role for the resulting approximate solution. Here, in this discrete mechanics approach, they are derived via a discrete variational principle, leading to structure preservation (symplecticity, consistency in momentum maps in the presence of symmetry and good energy behaviour) along the discrete trajectories, see [9, 6, 7].

Consider a time interval $[t_0, t_N] \subset \mathbb{R}$ and an equidistant grid $\{t_0, \ldots, t_n = t_0 + n\Delta t, \ldots, t_N\}$ based on the time step $\Delta t \in \mathbb{R}$ and a discrete configuration trajectory $\boldsymbol{q}_d = \{\boldsymbol{q}_n\}_{n=0}^N$ approximating the real configuration $\boldsymbol{q} : [t_0, t_N] \to Q$ in a configuration manifold $Q \subseteq \mathbb{R}^n$, i.e. $\boldsymbol{q}_n \approx \boldsymbol{q}(t_n)$. Furthermore, let the motion be constrained by m holonomic scleronomic constraints $\boldsymbol{g} : Q \to \mathbb{R}^m$ to the $(n-m)$-dimensional constraint manifold $C = \{\boldsymbol{q} \in Q | \boldsymbol{g}(\boldsymbol{q}) = \boldsymbol{0}\}$ and let $\boldsymbol{u}_d = \{\boldsymbol{u}_n\}_{n=0}^N$ with $\boldsymbol{u}_n \in U \subseteq \mathbb{R}^{n-m}$ denote a sequence of discrete generalised incremental coordinates such that the discrete nodal reparametrisation $\boldsymbol{F} : U \times Q \to C$ yields $\boldsymbol{q}_{n+1} = \boldsymbol{F}(\boldsymbol{u}_{n+1}, \boldsymbol{q}_n) \in C$. The degrees of freedom are actuated by the discrete control sequence $\boldsymbol{\tau}_d = \{\boldsymbol{\tau}_n\}_{n=0}^{N-1}$, approximating the control trajectory $\boldsymbol{\tau}(t) : [t_0, t_N] \to \mathbb{R}^{n-m}$ by a constant $\boldsymbol{\tau}_n \in \mathbb{R}^{n-m}$ in each time interval $[t_n, t_{n+1}]$. Using $\boldsymbol{\tau}_{n-1}^+ = \frac{\Delta t}{2}\boldsymbol{\tau}_{n-1}$ and $\boldsymbol{\tau}_n^- = \frac{\Delta t}{2}\boldsymbol{\tau}_n$, redundant n-dimensional control forces $\boldsymbol{B}^T(\boldsymbol{q}_n) \cdot (\boldsymbol{\tau}_{n-1}^+ + \boldsymbol{\tau}_n^-)$ can be computed using the configuration dependent input transformation matrix $\boldsymbol{B}^T(\boldsymbol{q}_n) \in \mathbb{R}^{n\times(n-m)}$. Finally, a null space matrix $\boldsymbol{P}(\boldsymbol{q}_n) : \mathbb{R}^{n-m} \to T_{\boldsymbol{q}_n}C$ spans the tangent space to the constraint manifold at the configuration $\boldsymbol{q}_n \in C$.

As usual in discrete mechanics, a discrete Lagrangian $L_d : Q \times Q \to \mathbb{R}$ approximates the action in a time interval, thus the action integral in the time continuous setting is transformed into a discrete action sum. Analoguous to Hamilton's principle, here a discrete variational principle requires stationarity of the discrete action. In the presence of non conservative actuation forces and constraints, a discrete constrained Lagrange-d'Alembert principle yields the variational integrator – in this case the constrained forced discrete Euler-Lagrange equations, where D_1L_d, D_2L_d denote differentiation of the discrete Lagrangian with

respect to the first and second arguments respectively. Using the discrete null space method with nodal reparametrisation, they are reduced to their minimal dimension. Altogether, discrete mechanics and optimal control for constrained systems (DMOCC) yields the following finite dimensional constrained optimisation problem for the simulation of the optimal control problem with boundary values $(\boldsymbol{q}(t_0), \dot{\boldsymbol{q}}(t_0)) = (\boldsymbol{q}^0, \dot{\boldsymbol{q}}^0)$ and $(\boldsymbol{q}(t_N), \dot{\boldsymbol{q}}(t_N)) = (\boldsymbol{q}^N, \dot{\boldsymbol{q}}^N)$. Note that J_d, C_d are discrete approximations to the objective and const functionals, respectively, while $\boldsymbol{s}_d, \boldsymbol{h}_d, \boldsymbol{r}_d$ are discrete versions of the initial, final and path contraints.

Let the contact constraint function be denoted by $g_c : Q \to \mathbb{R}$ and assume that it is computed as the solution of the LCLP. Then collision avoidance requires to augment DMOCC by the inequality constraint $g_c(\boldsymbol{q}_n) > 0$ for $n = 1, \ldots, N-1$.

DMOCC with collision avoidance
minimise discrete objective function

$$\min_{\boldsymbol{u}_d, \boldsymbol{\tau}_d} \quad J_d(\boldsymbol{u}_d, \boldsymbol{\tau}_d) = \min_{\boldsymbol{u}_d, \boldsymbol{\tau}_d} \quad \sum_{n=0}^{N-1} C_d(\boldsymbol{u}_n, \boldsymbol{u}_{n+1}, \boldsymbol{\tau}_n)$$

subject to the constraints for $n = 1, \ldots, N-1$

discrete equations of motion $\boldsymbol{P}^T(\boldsymbol{q}_n) \cdot \left[D_1 L_d(\boldsymbol{q}_n, \boldsymbol{F}(\boldsymbol{u}_{n+1}, \boldsymbol{q}_n)) + D_2 L_d(\boldsymbol{q}_{n-1}, \boldsymbol{q}_n) + \boldsymbol{B}^T(\boldsymbol{q}_n) \cdot \left(\boldsymbol{\tau}_{n-1}^+ + \boldsymbol{\tau}_n^- \right) \right]$	$=$	$\mathbf{0}$
collision avoidance	$g_c(\boldsymbol{q}_n)$	$>$	0
initial value constraints	$\boldsymbol{s}_d(\boldsymbol{u}_0, \boldsymbol{u}_1, \boldsymbol{\tau}_0, \boldsymbol{q}^0, \dot{\boldsymbol{q}}^0)$	$=$	$\mathbf{0}$
path constraints	$\boldsymbol{h}_d(\boldsymbol{u}_n, \boldsymbol{u}_{n+1}, \boldsymbol{\tau}_n)$	$\leq$	$\mathbf{0}$
final point constraints	$\boldsymbol{r}_d(\boldsymbol{u}_{N-1}, \boldsymbol{u}_N, \boldsymbol{\tau}_{N-1}, \boldsymbol{q}^N, \dot{\boldsymbol{q}}^N)$	$=$	$\mathbf{0}$

The constrained optimisation problem is solved in Matlab using the fmincon function (SQP algorithm with active set strategy or interior point method).

2.3 Example: puzzle assembly with collision avoidance

The considered puzzle consists of three non-smooth non-convex rigid bodies that are initially at rest in fully specified initial configurations. All bodies are fully actuated and supposed to reconfigure such that at the final time $t_N = 0.29$ (where $\Delta t = 0.01$ and $N = 29$), they are in a prescribed relative placement and orientation to each other. In other words, the puzzle manoeuvre ends at rest in a fully assembled configuration whose absolute placement and orientation in space is left free. During the manoeuvre, contact is detected using the SSHLP described in Section 2.1 and collisions are avoided. The initial guess for the optimisation is determined via an inverse dynamics problem, i.e. collision free reconfiguration trajectories have been guessed for the three bodies and the corresponding actuation has been determined solving the discrete equations of motion (see DMOCC with collision avoidance in Section 2.2) for the discrete control sequence $\boldsymbol{\tau}_d$. The goal of the optimisation is to minimise the control effort, i.e. $C_d = \Delta t \boldsymbol{\tau}_n^T \cdot \boldsymbol{\tau}_n$ while bounds on the optimisation variables $\boldsymbol{u}_d, \boldsymbol{\tau}_d$ ensure that a local minimum with relatively small displacements is found. The control effort is reduced from a value of $J_d = 89$ at the initial guess to $J_d = 0.0630$ for the optimised solution. See Figure 2 for snapshots of different configurations during the puzzle's assembly.

3 OPTIMAL CONTROL PROBLEMS WITH CONTACTS

In many optimal control tasks like e.g. docking manoeuvres or walking and jumping motion, contact can not be avoided or is even necessary. However, in most cases, it is not known in advance when or where contact takes place. In particular, one can optimise the contact time and configuration with respect to specified goals.

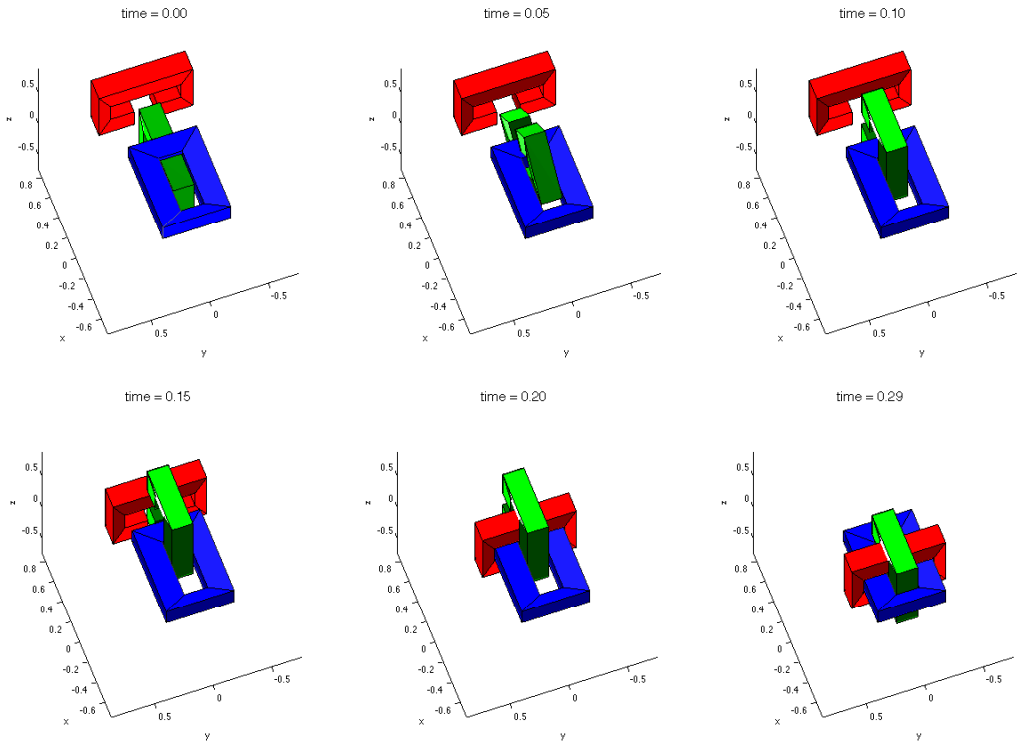

Figure 2. Puzzle assembly with collision avoidance: snapshots of different configurations.

3.1 Smooth penalty formulation

A penalty potential is an easy way to treat contact without loosing the generality of the problem formulation while retaining its smoothness, i.e. in DMOCC with collision avoidance described in Section 2.2, the collision avoidance inequality condition is left away. In case that the bodies overlap, i.e. $g_c(\boldsymbol{q}_n) < 0$, an n-dimensional penalty force $\boldsymbol{f}_n^c = \nabla(\frac{\mu}{2} g_c^2(\boldsymbol{q}_n))$ with the positive penalty parameter $\mu \in \mathbb{R}$ is included in the discrete equations of motion in DMOCC, which then read

$$\boldsymbol{P}^T(\boldsymbol{q}_n) \cdot \left[D_1 L_d(\boldsymbol{q}_n, \boldsymbol{F}(\boldsymbol{u}_{n+1}, \boldsymbol{q}_n)) + D_2 L_d(\boldsymbol{q}_{n-1}, \boldsymbol{q}_n) + \boldsymbol{B}^T(\boldsymbol{q}_n) \cdot \left(\boldsymbol{\tau}_{n-1}^+ + \boldsymbol{\tau}_n^- \right) + \boldsymbol{f}_n^c \right] = \boldsymbol{0}$$

Note that an explicit expression for the subderivative of the SSHLP can be readily evaluated such that ∇g_c can always be computed.

3.2 Non-smooth contact formulation

Suppose that a mechanical system is to be optimally controlled from an initial to a final state in such a way that precisely one collision takes place during the manoeuvre at a time node, say at $t_\iota \in [t_0, t_N]$ with $g_c(\boldsymbol{q}_\iota) = 0$. If the physical contact time was prescribed, the problem formulation would loose its generality. To retain generality, we let the contact time be determined as an optimisation variable. One way to realise this is to introduce positive scaling factors $\sigma_1, \sigma_2 \in \mathbb{R}$ for the time step before and after the contact time, see Figure 3. To ensure that time steps do not degenerate, the scaling factors can be bounded in the path constraints. Furthermore, the total manoeuvre time $t_N = (\iota\sigma_1 + (N - \iota)\sigma_2)\Delta t$ can either be left free, or bounded or fixed by a scalar valued function $w(\sigma_1, \sigma_2, t_N) \leq 0$ as desired.

The most crucial point in treating the contact is to determine the correct change in momentum due to the collision. Lets first assume that the collision is perfectly elastic and frictionless, i.e. the kinetic energy (and therewith the total energy) does not change when computed immediately before and after the impact. When a point mass hits a surface, its linear momentum component in the direction of the surface normal

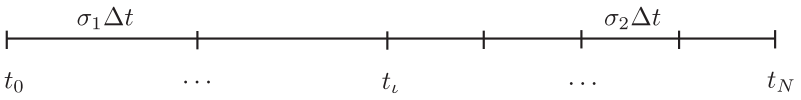

Figure 3. Time grid with differently scaled time step $\sigma_1\Delta t$ and $\sigma_2\Delta t$ before and after the contact time node t_ι.

at the contact point is reversed while the tangential component remains unchanged. However, the present situation is more complex since we deal with systems of rigid bodies having translational and rotational degrees of freedom on the one hand, and on the other hand, their kinematics is described using a constrained formulation reflecting their rigidity and possible interconnections by joints. These configuration constraints give rise to hidden constraints on velocity and on momentum level. Using the following discrete reduced Legendre transforms

$$\begin{aligned} {}^P\boldsymbol{p}_n^- =& \boldsymbol{P}^T(\boldsymbol{q}_n) \cdot \left[-D_1 L_d(\boldsymbol{q}_n, \boldsymbol{F}(\boldsymbol{u}_{n+1}, \boldsymbol{q}_n)) - \boldsymbol{B}^T(\boldsymbol{q}_n) \cdot \boldsymbol{\tau}_n^-\right] \\ {}^P\boldsymbol{p}_n^+ =& \boldsymbol{P}^T(\boldsymbol{q}_n) \cdot \left[D_2 L_d(\boldsymbol{q}_{n-1}, \boldsymbol{q}_n) + \boldsymbol{B}^T(\boldsymbol{q}_n) \cdot \boldsymbol{\tau}_{n-1}^+\right] \end{aligned}$$

the discrete equations of motion in DMOCC can be interpreted as ${}^P\boldsymbol{p}_n^+ - {}^P\boldsymbol{p}_n^- = \boldsymbol{0}$ which is a balance of discrete momenta at t_n, where the discrete momenta have been computed from the past (${}^P\boldsymbol{p}_n^+$) and the following time interval (${}^P\boldsymbol{p}_n^-$), respectively, and both are mapped by the null space matrix into the appropriate reduced cotangent space (being consistent with the constraints on momentum level). When a contact configuration has been reached, i.e. $g_c(\boldsymbol{q}_\iota) = 0$, the component of ${}^P\boldsymbol{p}_\iota^+$ in the direction of the surface normal has to be reflected. Note that in the reduced formulation, this surface normal is given by $\left({}^P\nabla g_c(\boldsymbol{q}_\iota)\right)^T = \boldsymbol{P}^T(\boldsymbol{q}_\iota) \cdot (\nabla g_c(\boldsymbol{q}_\iota))^T$. Thus, using the reduced mass matrix ${}^P\boldsymbol{M}(\boldsymbol{q}_\iota) = \boldsymbol{P}^T(\boldsymbol{q}_\iota) \cdot \boldsymbol{M} \cdot \boldsymbol{P}(\boldsymbol{q}_\iota)$ the component of ${}^P\boldsymbol{p}_\iota^+$ in the direction of the surface tangent, denoted by $\left({}^P\boldsymbol{p}_\iota^+\right)_\parallel$, fulfills

$$\left\langle \left({}^P\nabla g_c(\boldsymbol{q}_\iota)\right)^T, \left({}^P\boldsymbol{p}_\iota^+\right)_\parallel \right\rangle_{({}^P\boldsymbol{M}(\boldsymbol{q}_\iota))^{-1}} = 0 \tag{1}$$

where $\langle \boldsymbol{a}, \boldsymbol{b} \rangle_{\boldsymbol{A}} = \boldsymbol{a}^T \cdot \boldsymbol{A} \cdot \boldsymbol{b}$ is a norm for the vectors $\boldsymbol{a}, \boldsymbol{b}$ and the square matrix $\boldsymbol{A}$ of appropriate dimension. Inserting the momentum decomposition into the tangential and the normal direction ${}^P\boldsymbol{p}_\iota^+ = \left({}^P\boldsymbol{p}_\iota^+\right)_\parallel + \left({}^P\boldsymbol{p}_\iota^+\right)_\perp$ into Equation (1), the normal momentum component can be found explicitly via

$$\left({}^P\boldsymbol{p}_\iota^+\right)_\perp = \frac{\left\langle \left({}^P\nabla g_c(\boldsymbol{q}_\iota)\right)^T, {}^P\boldsymbol{p}_\iota^+ \right\rangle_{({}^P\boldsymbol{M}(\boldsymbol{q}_\iota))^{-1}}}{\left\langle \left({}^P\nabla g_c(\boldsymbol{q}_\iota)\right)^T, \left({}^P\nabla g_c(\boldsymbol{q}_\iota)\right)^T \right\rangle_{({}^P\boldsymbol{M}(\boldsymbol{q}_\iota))^{-1}}} \left({}^P\nabla g_c(\boldsymbol{q}_\iota)\right)^T$$

Finally, for frictionless collisions with a coefficient of restitution $e \in [0, 1]$, where $e = 1$ represents a perfectly elastic and $e = 0$ a perfectly plastic collision, the post collision momentum can be computed according to the following momentum reflection in normal direction at the contact surface

$${}^P\boldsymbol{p}_{\iota,post}^+ = {}^P\boldsymbol{p}_{\iota,pre}^+ - (1+e)\left({}^P\boldsymbol{p}_{\iota,pre}^+\right)_\perp$$

With these preliminaries, the DMOCC with contact problem can be formulated as folows.

DMOCC with contact
minimise discrete objective function

$$\min_{\boldsymbol{u}_d,\boldsymbol{\tau}_d,\sigma_1,\sigma_2} \quad J_d(\boldsymbol{u}_d,\boldsymbol{\tau}_d,\sigma_1,\sigma_2) = \min_{\boldsymbol{u}_d,\boldsymbol{\tau}_d} \quad \sum_{n=0}^{N-1} C_d(\boldsymbol{u}_n,\boldsymbol{u}_{n+1},\boldsymbol{\tau}_n,\sigma_1,\sigma_2)$$

subject to constraints for $n = 1,\dots,N-1$

discrete equations of motion	${}^P\boldsymbol{p}_n^+ - {}^P\boldsymbol{p}_n^-$	$=$	$\mathbf{0}$
contact	$g_c(\boldsymbol{q}_\iota)$	$=$	0
momentum reflection	${}^P\boldsymbol{p}_{\iota,pre}^+ - (1+e)\left({}^P\boldsymbol{p}_{\iota,pre}^+\right)_\perp$	$=$	${}^P\boldsymbol{p}_{\iota,post}^+$
initial value constraints	$\boldsymbol{s}_d(\boldsymbol{u}_0,\boldsymbol{u}_1,\boldsymbol{\tau}_0,\boldsymbol{q}^0,\dot{\boldsymbol{q}}^0)$	$=$	$\mathbf{0}$
path constraints	$\boldsymbol{h}_d(\boldsymbol{u}_n,\boldsymbol{u}_{n+1},\boldsymbol{\tau}_n,\sigma_1,\sigma_2)$	$\leq$	$\mathbf{0}$
final point constraints	$\boldsymbol{r}_d(\boldsymbol{u}_{N-1},\boldsymbol{u}_N,\boldsymbol{\tau}_{N-1},\boldsymbol{q}^N,\dot{\boldsymbol{q}}^N)$	$=$	$\mathbf{0}$
total time condition	$w(\sigma_1,\sigma_2,t_N)$	$\leq$	0

In particular, collision avoidance can be required at all other time nodes in the path constraints vector. If multiple, say $N_c \in \mathbb{N}$, collisions are planned at the time node numbers $\iota_1,\dots,\iota_{N_c}$, then multiple contact conditions $g_c(\boldsymbol{q}_{\iota_1}) = 0,\dots,g_c(\boldsymbol{q}_{\iota_{N_c}}) = 0$ with the corresponding momentum reflection conditions are constraining the optimisation in DMOCC with contact. Furthermore, $N_c + 1$ scaling factors are present in the total time condition $w(\sigma_1,\dots,\sigma_{N_c+1},t_N) \leq 0$.

ι	4	9	14
σ_1	2.1795	0.9653	0.6186
σ_2	0.8185	1.0149	1.3337
t_ι	0.2180	0.2172	0.2165
J_d	$1.0244 \cdot 10^{-6}$	$1.0194 \cdot 10^{-6}$	$1.0005 \cdot 10^{-6}$

Table 1. Cube hitting a wall: values of scaling factors, contact time and control effort for different contact node numbers ι.

3.3 Example: cube hitting the wall

In the first example, a cube starts in a prescribed initial state with a translational velocity towards a close by wall. In the prescribed final state, the final velocity is reversed and bounds on the actuation are set such that the final state can not be reached without a collision of the cube with the wall. Here, $N = 30$ time nodes and a time step of $\Delta t = 0.025$ are used and the control effort is minimised. The final time is prescribed as $t_N = 0.75$. This example serves as numerical evidence that the resulting optimal state and control trajectories and the resulting optimal contact time are independent of the chosen contact node number. Table 1 and Figure 4 shows that for $\iota \in \{4, 9, 14\}$ qualitatively the same contact time, control effort and evolution of actuating force and torque are obtained (of course the scaling factors yielding this contact time are different).

3.4 Example: two cubes with two planned collisions

The following problem considers two cubes with fully specified initial configurations. The green cube is initially at rest. It is not actuated, thus its final state is not prescribed. The blue cube has an initial velocity and is required to be steered into a prescribed final rest position that overlaps with the green cube's initial configuration. Thus, the blue cube must push the green cube out of the way, wherefore two collisions are planned at the time node numbers $\iota_1 = 20, \iota_2 = 39$ and collisions are avoided at all other time nodes. Altogether, $N = 50$ time nodes and $\Delta t = 0.01$ are used, while the final time is prescribed as $t_N = 0.5$, thus the total time condition $w(\sigma_1,\sigma_2,\sigma_3,t_N) = (\sigma_1\iota_1 + \sigma_2(\iota_2 - \iota_1) + \sigma_3(N - \iota_2))\Delta t - t_N = 0$ is used in DMOCC with contact described in Section 3.2. As a result of the control problem minimising the control effort to $J_d = 2.8573 \cdot 10^{-5}$, collisions happen at $t_{\iota_1} = 0.1975$, $t_{\iota_2} = 0.3900$, thus $\sigma_1 = 0.98725, \sigma_2 =$

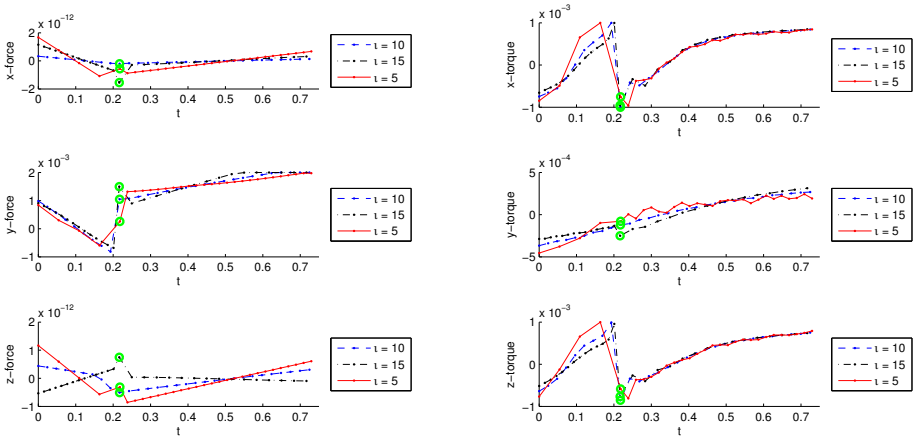

Figure 4. Cube hitting a wall: evolution of actuating force and torque for different contact node numbers ι. The contact time is marked in green.

$1.0132, \sigma_3 = 1.0004$. The initial guess for the optimisation is obtained via a forward dynamics simulation (treating contact according to the decomposition contact response formulation given in [1], which has been extended for the case of oriented bodies and constrained dynamics) yielding also a guess for possible contact times. The left hand side plot in Figure 5 shows the evolution of the actuating force and torque for the blue cube. The corresponding net torque evolution as well as the evolution of angular momentum for the complete system are shown in the right hand side plot, where the lowest plot shows the consistency of the angular momentum evolution, i.e. the change in angular momentum exactly represents the actuation (up to the numerical tolerance) giving numerical evidence of the structure preservation properties of the discrete equations of motion. Snapshots of different configurations are depicted in Figure 6.

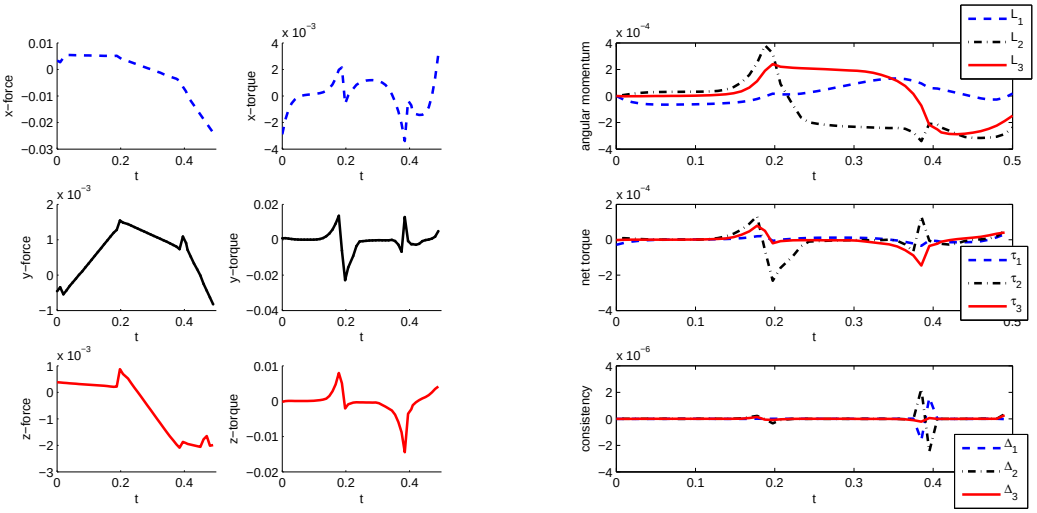

Figure 5. Two cubes with two planned collisions: evolution of actuating force and torque on blue cube (left) and evolution of angular momentum, net torque and consistency of angular momentum for the complete system (right).

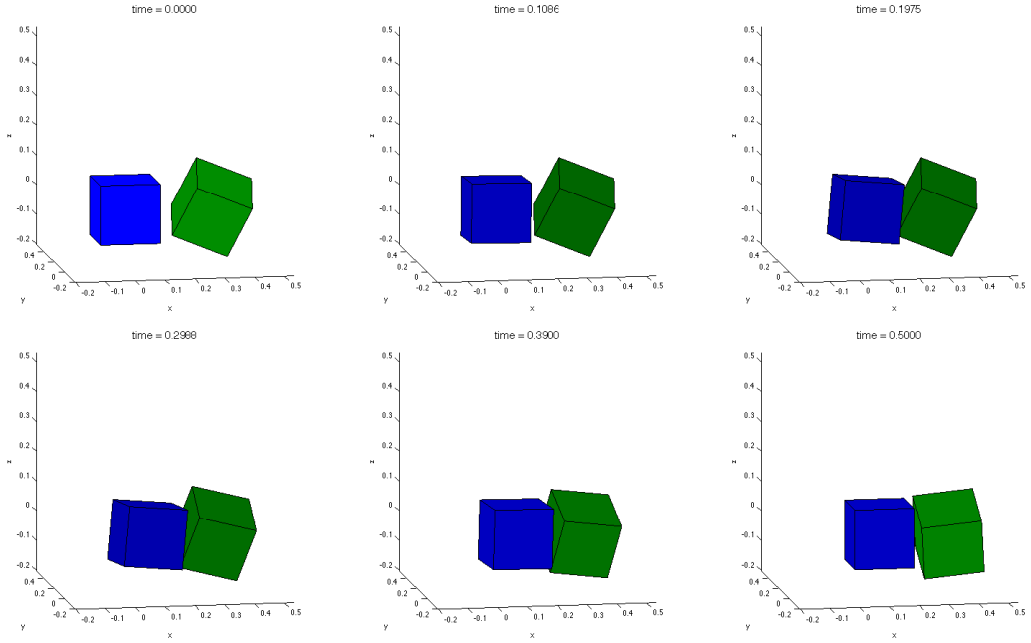

Figure 6. Two cubes with two planned collisions: snapshots of different configurations.

4 CONCLUSIONS

With the supporting separating hyperplane linear programming (SSHLP) approach, a very efficient method for detecting contact between non-smooth bodies has been described briefly. The resulting signed distance between the bodies is first of all used as an inequality constraint in optimal control simulations with collision avoidance. Secondly, optimal control manouevres with planned contacts and collisions are considered. Here it is an advantage that the subgradient of the SSHLP, supplying the direction of the contact force, can be readily evaluated. For the simulation of contact manoeuvres, the time grid is variable, such that the contact time can be determined as part of the optimisation while the contact node number can be fixed, what fascilitates the implementation substantially. The presented formulation and results constitute first steps of ongoing work and many theoretical aspects and more complex examples will be considered in the future. Furthermore, a comparison of the SSHLP's efficiency with standard contact detection methods is required.

REFERENCES

[1] Cirak, F.; West, M.: Decomposition contact response (DCR) for explicit finite element dynamics. Int. J. Numer. Meth. Engng., Vol. 64, No. 3, pp. 1078–1110, 2005.

[2] Fetecau, R.C.; Marsden, J.E.; Ortiz, M; West, M.: Nonsmooth Lagrangian mechanics and variational collision integrators. Siam J. applied dynamical systems, Vol. 2, No. 3, pp. 381–416, 2003.

[3] Glocker, C.: Scalar force potentials in rigid multibody systems. Multibody Dynamics with Unilateral Contacts, CISM Courses and Lectures, Vol. 421, pp. 69–146, 2000.

[4] Johnson, G.; Ortiz, M.; Leyendecker, S.: A linear programming-based algorithm for the signed separation of (non-smooth) convex bodies. Submitted for publication, 2011.

[5] Leine, R.I.; van Campen, D.H.; Glocker, C.: Nonlinear dynamics and modeling of various wooden toys with impact and friction. Journal of vibration and control, Vol. 9, No. 3, pp. 25–78, 2003.

[6] Leyendecker, S.; Marsden, J.E.; Ortiz, M.: Variational integrators for constrained dynamical systems. Zeitschrift für Angewandte Mathematik und Mechanik, Vol. 88, No. 9, pp. 677–708, 2008.

[7] Leyendecker, S.; Ober-Blöbaum, S.; Marsden, J.E.; Ortiz, M.: Discrete mechanics and optimal control for constrained systems. Optimal Control Applications & Methods, Vol. 31, No. 6, pp. 505–528, 2010.

[8] Leyendecker, S.; Hartmann, C.; Koch, M.: Variational collision integrator for polymer chains. J. Comput. Phys., Vol. 231, pp. 3896–3911, 2012.

[9] Marsden, J.E.; West, M.: Discrete mechanics and variational integrators. Optimal Control Applications & Methodsk, Vol. 31, No. 6, pp. 505–528, 2010.

[10] Pandolfi, A.; Kane, C.; Marsden, J.E.; Ortiz, M.: Time-discretized variational formulation of nonsmooth frictional contact. Acta Numerica, Vol. 10, pp. 357–514, 2001.

[11] Pang, J.S.; Trinkle, J.C.: Complementarity formulations and existence of solutions of dynamic multi-rigid-body contact problems with Coulomb friction. Math. Program., Vol. 73, pp. 119–226, 1996.